

# Quick Approximation of Camera's Spectral Response from Casual Lighting

Dilip K. Prasad   Rang Nguyen   Michael S. Brown  
School of Computing, National University of Singapore

dilip@comp.nus.edu.sg | nguyenho@comp.nus.edu.sg | brown@comp.nus.edu.sg

## Abstract

Knowing the RGB spectral sensitivities of a camera is useful for several image processing applications. However, camera manufacturers seldom provide this information. Calibration methods for determining them can be daunting, requiring either sophisticated instruments or carefully controlled lighting. This paper presents a quick and easy method that provides a reasonable approximation of the camera response functions with only a color chart and casual unknown illuminations. Our approach is enabled by careful design of the cost function that imposes several constraints on the problem to make it tractable. In the components of the cost function, the Luther condition provides the global shape prior and the commercial lighting systems with unknown spectra provide narrow spectral windows for local reconstruction. The quality of reconstruction is comparable with other methods that use known illumination.

## 1. Introduction and Background

While RGB images are the defacto standard format used in most computer vision and image processing algorithms, the images are formed from a more complex description of the scene in the spectral domain. In particular, RGB images are formed by the integration of the spectral illumination, spectral reflectivities of the scene, and the spectral response of the camera itself. The integration can be considered as a projection onto the camera's spectral sensitivity at each color channel (R, G, B). As a result, the resulting RGB image is a spectral intermingling of the surface materials and the environment lighting that is difficult to resolve without prior knowledge of the scene and lighting.

Nevertheless, the knowledge of spectral response of the camera can be useful for several applications, like computational color constancy [2, 9], scene classification, and spectral tweaking of the scenes. Unfortunately, manufacturers rarely reveal the camera response functions. As a result, they must be determined through calibration approaches, for which several high-end methods have been developed (e.g. see [8, 13, 12]). These methods use special equip-

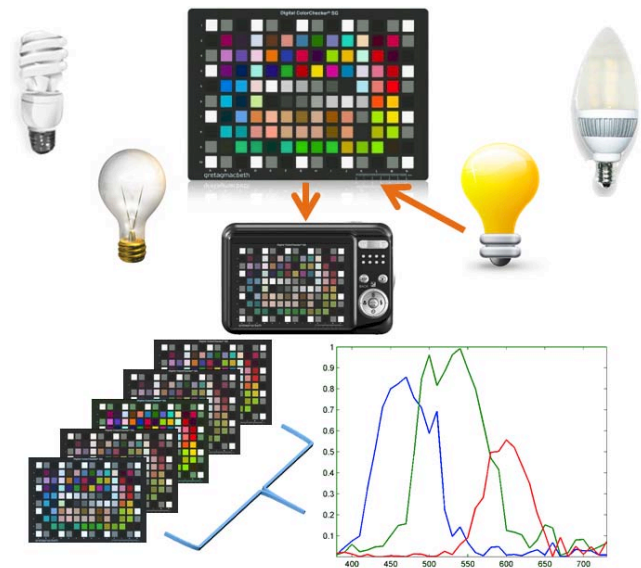


Figure 1. Reconstructing camera response functions from casual lighting

ment setup such as monochromator and spectrophotometer. While these approaches are successful, they are limited to a lab environment, making it impractical for widespread application or incorporation in commercial image processing tools.

Other methods use a color chart and controlled illumination (e.g. [11, 6]). However, determining the illumination spectrum is another time consuming and costly spectral measurement problem and assuming loosely defined conditions like day light illumination may introduce its own error or complications. To overcome this issue, some researchers proposed the use of special targets like LED based emissive targets [3] and fluorescence targets [5]. However, their use is still restrictive due to high cost and precise fabrication requirements. A recent method [9] estimates the camera spectral response by using precomputed mathematical basis from sky model database to predict sky spectrum from general images containing sky in the scene while assuming the geolocation of the captured sky is precisely known.

This paper attempts to make the estimation of camera

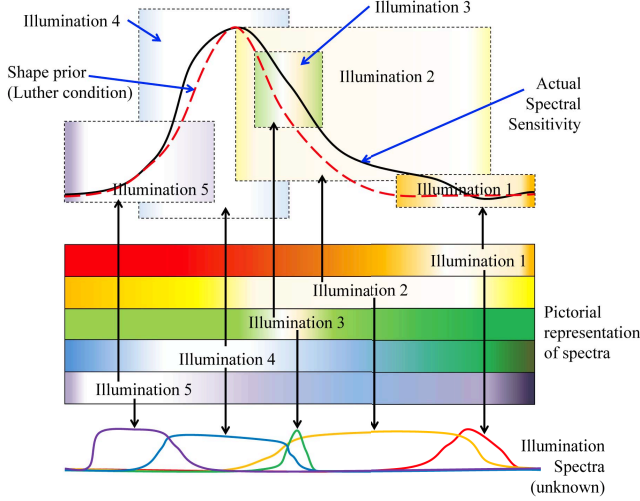


Figure 2. Reconstruction of spectral sensitivity - an illustration.

sensitivity response easier. In particular, we show that the camera response functions can be reconstructed using a few images of the MacBeth ColorChecker Digital SG taken under diverse unknown illuminations. The issue of the inherent low dimensionality of cameras' color space [3, 6, 7, 10] earlier implied that the reconstruction is restrictive. To tackle this, [11] suggested to take multiple images of the target using different LED illumination spectra with known spectral properties. On the contrary, our method does not need the illumination spectrum.

**Our Contribution:** Our work is different since we consider general off-the-shelf available light sources, the spectra of which are unknown (not available). The only assumption is that the illuminations are chosen such that together they cover the entire visible spectrum while each of them has a different spectrum. For example, in this paper, we have chosen commercial light sources of five varieties: fluorescent cool light, fluorescent warm light, incandescent bulb, halogen light, and light emitting diodes. Though their spectra are not available, it is easy to predict that they are spectrally different and span the entire visible spectrum as well. Our method can be explained using an analogy of a panoramic scene of a mountain being viewed from a room. Each illumination provides a window into the spectral response function, and together with the shape prior imposed by Luther condition, they provide the whole panoramic view of the spectral response function. This is pictorially illustrated in Fig. 2.

The paper is organized as follows. Section 2 details our approach and the optimization strategy. In section 3, our results are compared with other methods and the true spectral sensitivities measured using spectral measurement setup [8]. Section 4 provides a discussion and summary of our work.

## 2. Calibration Method with Unknown Lighting

### 2.1. Problem modeling

According to the Lambertian model of camera [4], the color intensity measured by the camera sensors is given by:

$$I_{k,x}^{\{i\}} = \int C_k(\lambda) L^{\{i\}}(\lambda) R_x(\lambda) d\lambda, \quad k = R, G, B, \quad (1)$$

where  $I, k, x$  denote the normalized (divided by maximum value) color intensity, the color channels ( $R$  - red,  $G$  - green,  $B$  - blue), and the camera pixels (and the corresponding coordinate in the scene), respectively. Further,  $C_k(\lambda)$  denotes the camera sensor's response function for the  $k$ th channel,  $L^{\{i\}}(\lambda)$  denotes the illumination spectrum of the  $i$ th light source, and  $R_x(\lambda)$  denotes the scene reflectance.

In the discretized form, eq. (1) can be written as:

$$\mathbf{I}_k^{\{i\}} = \mathbf{R} \left( \mathbf{C}_k \odot \mathbf{L}^{\{i\}} \right), \quad (2)$$

where  $\mathbf{I}_k^{\{i\}}, \mathbf{C}_k$ , and  $\mathbf{L}^{\{i\}}$  are the vectors containing  $I_{k,x}^{\{i\}}, C_k(\lambda)$ , and  $L^{\{i\}}(\lambda)$  respectively.  $\mathbf{R}$  is a matrix containing the  $R_x(\lambda) d\lambda$  and the operator  $\odot$  represents element-wise multiplication. The vectors  $\mathbf{C}_k, k = R, G, B$  and  $\mathbf{L}^{\{i\}}$  are the unknowns with the constraint of being positive definite. For the MacBeth digital color checker, we have used the spectral reflectivities provided in the website [1]. For estimating these unknowns, denoted by  $\mathbf{C}_k$  and  $\mathbf{L}^{\{i\}}$ , we define the following residue functions:

$$\mathbf{e}_k^{\{i\}} = \left| \mathbf{I}_k^{\{i\}} - \mathbf{R} \left( \mathbf{C}_k \odot \mathbf{L}^{\{i\}} \right) \right| \quad (3)$$

$$\mathbf{f}_k = \frac{\left| \mathbf{x}_k - \mathbf{T}_k^T \mathbf{C}_k \right|}{\left| \mathbf{x}_k \right|}, \quad (4)$$

where  $\mathbf{T} = \left[ \mathbf{T}_R \quad \mathbf{T}_G \quad \mathbf{T}_B \right]^T$  is computed as:

$$\mathbf{T} = \left[ \mathbf{x}_R \quad \mathbf{x}_G \quad \mathbf{x}_B \right] \left[ \mathbf{C}_R \quad \mathbf{C}_G \quad \mathbf{C}_B \right]^\dagger. \quad (5)$$

Here, superscript  $\dagger$  represents matrix pseudoinverse and  $\left[ \mathbf{x}_R \quad \mathbf{x}_G \quad \mathbf{x}_B \right]$  represents the color matching functions of the CIE-1931 color matching functions. Eq. (4) represents the Luther condition which requires the cameras' response functions to be a linear combination of the CIE color matching functions. It is notable that the Luther condition is often weakly satisfied by the commercial camera systems [8].

We formulate a minimization problem as follows:

$$\begin{aligned} \min_{\{\mathbf{C}_k, \mathbf{L}^{\{i\}}\}} & : \left\{ \sum_{\forall i,k} \left( \mathbf{e}_k^{\{i\}} \right)^2 + \sum_{\forall k} \left( \mathbf{f}_k \right)^2 \right\}, \quad (6) \\ \text{s.t.} & : \mathbf{C}_k, \mathbf{L}^{\{i\}} \in [0, 1] \end{aligned}$$

and reconstruct the camera response functions.

## 2.2. Implication of the minimization problem

Note that minimizing eq. (3) for the  $i$ th light source is equivalent to optimizing the product  $\mathbf{C}_k \odot \mathbf{L}^{\{i\}}$  for that light source. Alternatively,  $\mathbf{C}_k \odot \mathbf{L}^{\{i\}}$  can be considered as viewing the function  $\mathbf{C}_k$  through a window function  $\mathbf{L}^{\{i\}}$ , which itself is unknown. Nevertheless, lighting conditions can be chosen such that each lighting condition provides a small clear view of the function  $\mathbf{C}_k$  and together they span the entire visible spectrum.

Most commercial lights do not have wide spectrum like daylight and different lights can be chosen to approximately focus on one or two portions of the spectrum. For example, we know that fluorescent warm light has large yellow spectral content while fluorescent cool light has peaks in the blue-green spectral region. Incandescent light's spectrum largely contains yellow-red components. LED lighting typically has a narrow band spectral response, and so on.

Then for a given commercial light source, minimizing eq. (3) requires a better reconstruction only in the spectral window(s) of that light source. Thus, the task of reconstructing  $\mathbf{C}_k$  is split into simpler tasks of reconstructing  $\mathbf{C}_k \odot \mathbf{L}^{\{i\}}$  in the spectrum of the  $i$ th light source's only.

On the other hand, residue in Luther condition, eq. 4, imposes that  $\mathbf{C}_k$  follows the approximate shape of the CIE spectral function irrespective of the value of  $\mathbf{C}_k \odot \mathbf{L}^{\{i\}}$ . In this way, each illumination contributes to the reconstruction of a part of  $\mathbf{C}_k$ , while the CIE spectral functions introduce the shape prior for  $\mathbf{C}_k$ . An illustration of the concept discussed above is shown in Fig. 2.

In other words, there are several equations that  $\mathbf{C}_k$  should satisfy, most being concentrated in the spectral spread of the light sources, and the Luther condition over the entire spectrum. This enables a good reconstruction of  $\mathbf{C}_k$ . On the other hand, each  $\mathbf{L}^{\{i\}}$  has only one residue per light source, which is not a linear function of  $\mathbf{C}_k$ . Thus, the reconstruction of  $\mathbf{L}^{\{i\}}$  is much more ill-posed than reconstruction of  $\mathbf{C}_k$ . As a result, it is unfair to expect that  $\mathbf{L}^{\{i\}}$  can be reconstructed correctly.

## 2.3. Optimization details

The minimization of the cost function in eq. (6) is a non-linear least squares problem and we are solving it with trust-region algorithm with its default settings in Matlab. The initial guess is generated by assigning random numbers in the range  $[0, 1]$  to all the unknowns. In general we consider the frequency range 380 nm to 730 nm, at a step of 10 nm. However, since the spectral reflectivities of all the patches in the color chart are very low in the low frequencies, sometimes, it results in unreasonable peaks in either the reconstruction of  $\mathbf{C}_k$  or  $\mathbf{L}_i$ . In such situations, we clip the first few frequency points and begin optimization from 410 nm. Typically, a few hundred iterations are sufficient for convergence. So, we fix the maximum number of iteration to 500.

Further, since the Luther condition is only weakly satisfied by the commercial cameras, we stop optimization if the value of the cost function falls below 0.2 (based on the error in satisfying Luther Condition being less than 0.2 for most cameras (Fig. 3 of [8])). The method takes  $\sim 1$  minute when implemented and executed on a i7-3770 CPU@3.4 GHZ, 16 GB, Windows 8 system using Matlab 2012a.

We note that the above optimization scheme may not be the best suitable and better scheme can be designed for better or faster convergence. Further, a smoothing or additional regularization scheme may help in producing smoother and less oscillatory reconstruction of the response functions. Here, for simplicity and conceptual development, we have not considered smoothing or regularization operations.

## 3. Reconstruction results and comparison

In this section, we show reconstruction results of the camera response functions for 28 cameras, which appear in the dataset provided in [8]. We compare our results with the actual spectral response functions (ground truth) presented in the dataset [8], and the reconstructions obtained by eigen bases [8], singular value decomposition bases, polynomial bases, radial basis functions, and fourier bases[13].

### 3.1. Brief summary of other methods

**Singular value decomposition (SVD):** Given the spectral response functions of several cameras ( $m = 1$  to  $M$ ) for a given channel  $k$ ,

$$\mathbf{C}_k = [C_k^1 \ C_k^2 \ \dots \ C_k^m \ \dots \ C_k^M]. \quad (7)$$

The singular value decomposition of the matrix  $\mathbf{C}$ ,

$$\mathbf{C} = [u_1 \ u_2 \ \dots \ u_N] \text{diag}([s_1 \ s_2 \ \dots \ s_M]) [v_1 \ v_2 \ \dots \ v_M]^T, \quad (8)$$

gives the statistical bases of the response function  $C_k$  in  $u_n$ . Here,  $N$  is the number of samples in frequency space. For  $s_1 \geq s_2 \geq \dots \geq s_M$ ,  $C_k$  can be approximated as:

$$C_k = \sum_{d=1}^D a_d u_d, \quad (9)$$

where  $D$  is the number of bases chosen and  $a_d$  are the coefficients to be determined.  $D = 2$  is used for generating the results [8].

**Principal component analysis (PCA):** Using the matrix  $\mathbf{C}$ , the principal component analysis is done by eigenvalue decomposition of  $\mathbf{C}\mathbf{C}^T$ :

$$\mathbf{C} = [e_1 \ e_2 \ \dots \ e_N] \text{diag}([\varepsilon_1 \ \varepsilon_2 \ \dots \ \varepsilon_N]) [e_1 \ e_2 \ \dots \ e_N]^T. \quad (10)$$

Then for  $\varepsilon_1 \geq \varepsilon_2 \geq \dots \geq \varepsilon_M$ ,  $C_k$  can be approximated as:

$$C_k = \sum_{d=1}^D a_d e_d, \quad (11)$$

where  $D$  is the number of bases chosen and  $a_d$  are the coefficients to be determined.  $D = 2$  is used for generating the results [8].

**Fourier bases (FB):** Let the camera response function of a camera be given by:

$$C_k = \sum_{d=1}^D a_d \sin(d\lambda\pi), \quad (12)$$

where  $\lambda$  ranges evenly from 0 to 1 ( $N$  samples),  $D$  is the number of bases chosen and  $a_d$  are the coefficients to be determined. Here  $f_d = \sin(d\lambda\pi)$  are the Fourier bases.  $D = 8$  is used for generating the results [13].

**Polynomial bases (PB):** Let the camera response function of a camera be given by:

$$C_k = \sum_{d=1}^D a_d (\lambda)^d, \quad (13)$$

where  $\lambda$  ranges evenly from 0 to 1 ( $N$  samples), where  $D$  is the number of bases chosen and  $a_d$  are the coefficients to be determined. Here  $p_d = (\lambda)^d$  are the polynomial bases.  $D = 8$  is used for generating the results [13].

**Radial basis functions (RBF):** Let the camera response function of a camera be given by:

$$C_k = \sum_{d=1}^D a_d \exp\left(-\frac{(\lambda - \mu_d)^2}{\sigma^2}\right), \quad (14)$$

where  $\lambda$  ranges evenly from 0 to 1 ( $N$  samples), where  $D$  is the number of bases chosen and  $a_d$  are the coefficients to be determined. Here  $r_d = \exp\left(-\frac{(\lambda - \mu_d)^2}{\sigma^2}\right)$  are the radial basis functions.  $D = 8$  is used for generating the results [13]. The means  $\mu_d$  are chosen as (0.3125, 0.3795, 0.4464, 0.5134, 0.5804, 0.6473, 0.7143, 0.7813) and  $\sigma$  is chosen as 0.125.

**Intensity computation for the other methods:** In all the other methods [8, 13], the spectrum of D65 illumination, the spectral reflectivities of Macbeth ColorChecker Digital SG [1], and the ground truth of the spectral response functions of a camera [8] are used to generate the intensity corresponding to each color patch in the color chart using the Lambertian model (eq. (1) and (2) of the main paper). 3% additive Gaussian noise is added to the intensity values to simulate the intensity variation often present in true images in the area of each patch.

**Computation of camera response function:** The bases functions are collected in the matrix  $\mathbf{B} =$

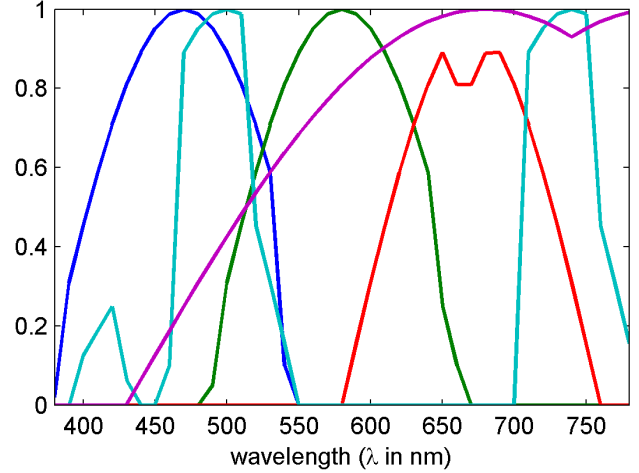


Figure 3. Illumination spectra of the sources considered in synthetic illumination experiment.

$[b_1 \ b_2 \ \dots \ b_D]$  and the coefficients of the bases in  $A = [a_1 \ a_2 \ \dots \ a_D]^T$ . Then the Lambertian model in eq. (1) can be written as:

$$\mathbf{I}_k^{\{i\}} = \mathbf{R} \text{diag}(\mathbf{L}_{D65}) \mathbf{B} A, \quad (15)$$

and  $A$  is derived as:

$$A = (\mathbf{R} \text{diag}(\mathbf{L}_{D65}) \mathbf{B})^\dagger \mathbf{I}_k^{\{i\}}, \quad (16)$$

where  $\mathbf{L}_{D65}$  is the spectrum of D65 lighting and  $\dagger$  denotes the pseudoinverse.

### 3.2. Experiments

We split our comparison into two parts: Real illumination experiment and synthetic illumination experiment.

**Real illumination experiment:** We had four cameras, Canon EOS 1D Mark III, Canon EOS 5D Mark II, Nikon D40, and Sony NEX-5N, which were included in the spectral response dataset in [8]. For each of these cameras, we took the pictures of the color chart in five different illuminations, which we roughly label as fluorescent cool light (FCL), fluorescent warm light (FWL), incandescent bulb (IB), halogen light (HL), and light emitting diodes (LED). The exact spectra of the light sources are unknown and the sources have been picked from general retail stores. The reconstructed color response functions for four cameras using the proposed method, the other methods, and the ground truth are shown in Fig. 4 and 5.

**Synthetic illumination experiment:** For the remaining 24 cameras in [8], five synthetic illuminations shown in Fig. 3 are considered. For each illumination, the intensity corresponding to each patch is computed using the Lambertian model (eq. (1) and (2)). 3% additive Gaussian noise is added to the intensity values to simulate the intensity variation often present in true images in the area of each patch.

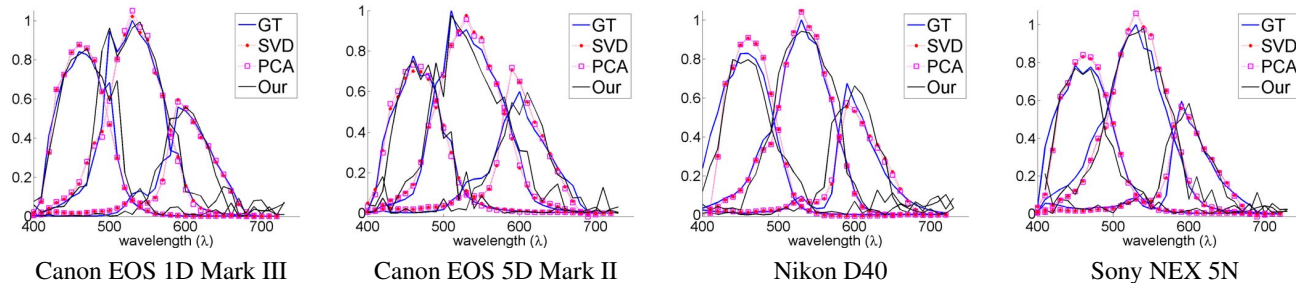


Figure 4. Comparison of reconstruction results of the proposed method (Our), other methods (SVD: singular value decomposition, PCA: principal component analysis), and the ground truth (GT) for the 4 cameras used in real illumination experiment.

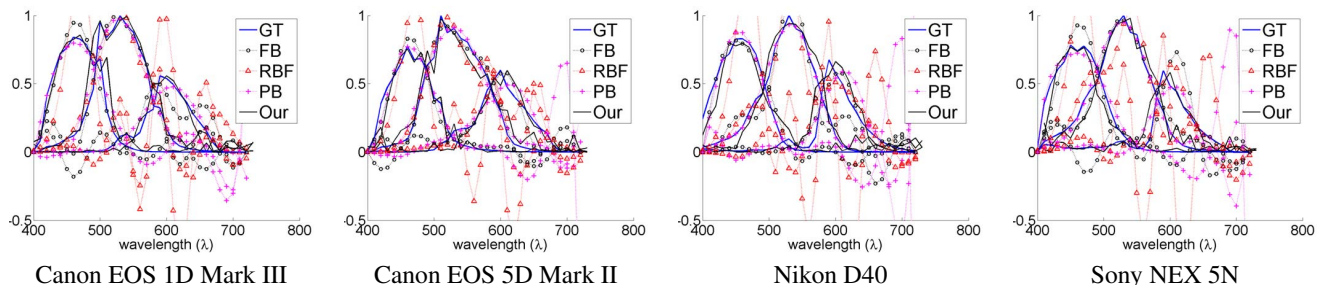


Figure 5. Comparison of reconstruction results of the proposed method (Our), other methods (FB: Fourier bases, RBF: radial basis functions, PB: polynomial bases), and the ground truth (GT) for the 4 cameras used in real illumination experiment. The span of vertical axis is kept between -0.5 and 1 for clarity of the plots.

Using these illuminations, the measured spectra of the cameras, and the spectral reflectivities of the patches in the color chart, we synthetically compute the expected intensity of each patch. These intensities are then used for reconstructing the spectral sensitivities of the camera. The comparison of the reconstructed spectral sensitivities, results of other methods, and the ground truth are shown in Fig. 6 and 7. The proposed method uses five unknown illumination conditions while the other methods [8, 13] assume D65 illumination condition.

### 3.3. Observations

The comparison of the proposed method (with unknown illuminations) with other methods (with known D65 illumination) is provided in Figs. 4 – 7. Further, for quantitative comparison, we define the reconstruction error of the  $k$ th channel as follows:

$$\text{err}_k = \sum (C_k \odot |C_k^{\text{true}} - C_k|), \quad (17)$$

where  $C_k^{\text{true}}$  is the true spectral sensitivity vector (ground truth) taken from the dataset of [8]. The statistics of the above reconstruction error for all the 28 cameras considered in this paper are plotted in Fig. 8.

In Figs. 5 and 7, it is seen that Fourier, RBF, and polynomial bases are more oscillatory and less accurate in representing the camera response functions. The lesser accuracy is verified in the error statistics plotted in Fig. 8 for

all the channels. In general, SVD and PCA bases are more accurate in representing the camera response functions, as verified in Figs. 4, 6, and 8. This effect is expected since these bases were derived statistically using the data collected from the same 28 cameras. The accuracy may be poorer if the concerned camera's response functions are not a part of this database of  $C_k$  [8]. Their accuracy for other cameras may be poorer. The proposed method represents the camera response reasonably well despite the illumination spectra being unknown, though it also demonstrates slight oscillations in the edges. Further, for some industrial cameras like Point Grey cameras (Fig. 6, last row), the proposed method is unable to represent the camera response functions well. It is interesting to note that for such cases, even the statistical PCA and SVD bases also result into poor reconstruction (see Fig. 6). We attribute poor accuracy of the proposed method for these cameras to their response functions satisfying the Luther condition very weakly (see Fig. 3 of [8]). Further, for the statistical bases, the accuracy for these cameras is poor because their deviation from other cameras in the database is very large. In essence, our method may perform poorer if the camera satisfies the Luther condition very weakly.

We highlight that in our method, no apriori information like the spectral dataset of the cameras or the illumination spectrum is used while other methods with orthogonal bases assume daylight condition, still our method shows more versatility and reasonable performance.

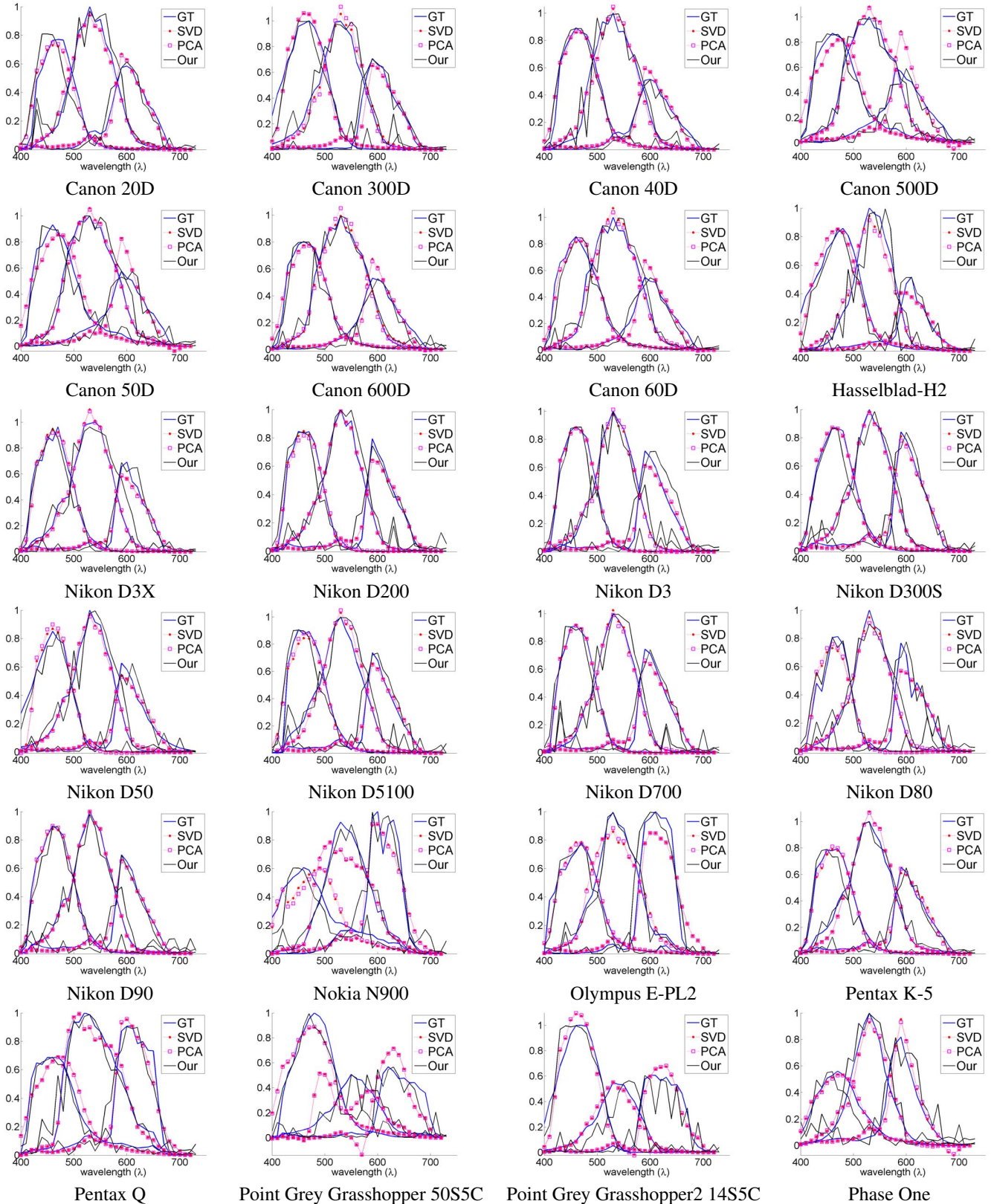


Figure 6. Comparison of reconstruction results of the proposed method (Our), other methods (SVD: singular value decomposition, PCA: principal component analysis), and the ground truth (GT) for the 24 cameras used in synthetic illumination experiment.

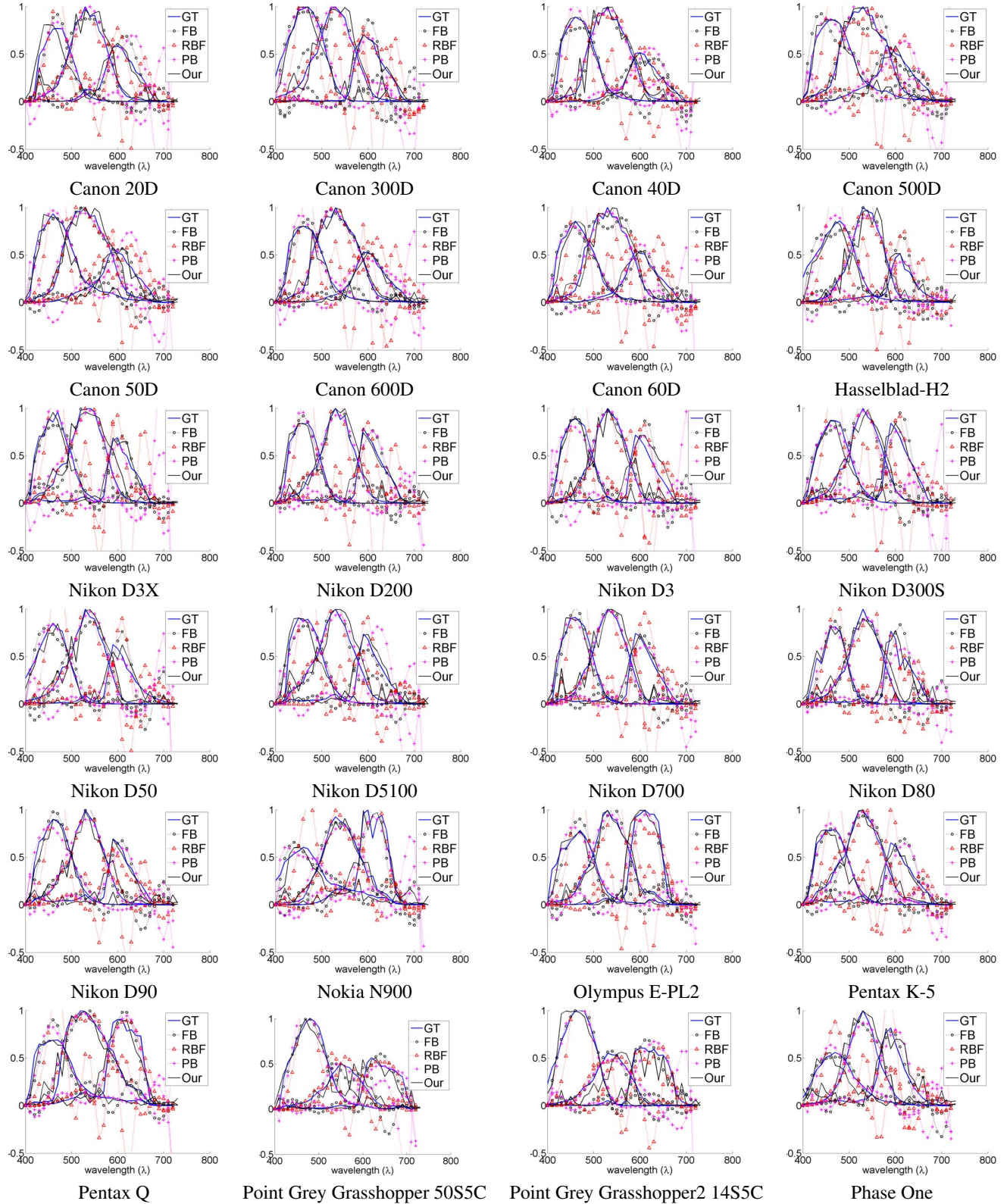


Figure 7. Comparison of reconstruction results of the proposed method (Our), other methods (FB: Fourier bases, RBF: radial basis functions, PB: polynomial bases), and the ground truth (GT) for the 24 cameras used in synthetic illumination experiment. The span of vertical axis is kept between -0.5 and 1 for clarity of the plots.

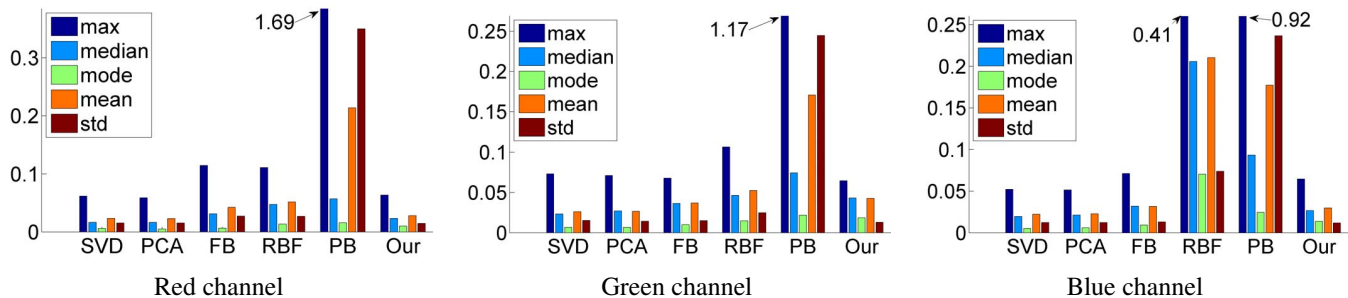


Figure 8. Reconstruction error statistics (for error defined in eq. 17) of the proposed and other methods for the three channels. max: maximum error, std: standard deviation. The data of max errors is clipped in some cases for better representation. The actual max errors are written in the text for such cases.

## 4. Discussion and Conclusion

Despite the popular belief that the camera spectral responsivities cannot be reconstructed well using images of only reflective color targets under unknown illuminations, we show that a reasonable reconstruction of the camera response functions is possible. In addition to the usually used linear difference equations, we incorporate Luther condition in the minimization problem, which introduces an indirect shape constraint while minimizing the other residues. On the other hand, the reconstruction task is distributed among various illuminations due to their inherent spectral characteristics even if the illumination spectra are unknown. In this manner, we show that cameras spectral responsivities can be estimated with reasonable accuracy using simple images of reflective color charts in few casual indoor lighting conditions without requiring sophisticated and expensive spectral lab facilities.

In the future, it shall be interesting to study whether the illumination spectrum can also be reconstructed well, though no apriori information about the camera and light source may be available. Subject to its accuracy, such illumination reconstruction may enable illumination engineering in the image processing realm. For example, it may allow photography community to artificially simulate the desired illumination conditions without sophisticated equipment.

## Acknowledgement

This work was supported by Singapore A\*STAR PSF grant 11212100.

## References

- [1] BabelColor. Spectral data of the ColorChecker Digital SG, 11th-Apr-2013.
- [2] K. Barnard, F. Ciurea, and B. Funt. Sensor sharpening for computational color constancy. *JOSA A*, 18(11):2728–2743, 2001.
- [3] J. M. DiCarlo, G. E. Montgomery, and S. W. Trovinger. Emissive chart for imager calibration. In *IS and T/SID Color Imaging Conference*, pages 295 – 301, 2004.
- [4] C. M. Goral, K. E. Torrance, D. P. Greenberg, and B. Bataille. Modeling the interaction of light between diffuse surfaces. In *ACM SIGGRAPH Computer Graphics*, volume 18, pages 213–222, 1984.
- [5] S. Han, I. Sato, T. Okabe, and Y. Sato. Fast spectral reflectance recovery using dlp projector. In *ACCV*, volume pt.1, pages 323 – 35, 2011.
- [6] J. Y. Hardeberg, H. Brettel, and F. J. Schmitt. Spectral characterization of electronic cameras. In *SYBEN-Broadband European Networks and Electronic Image Capture and Publishing*, pages 100–109, 1998.
- [7] P. Herzog, D. Knipp, H. Stiebig, and F. Konig. Colorimetric characterization of novel multiple-channel sensors for imaging and metrology. *J. Electron. Imaging*, 8(4):342 – 53, 1999.
- [8] J. Jiang, D. Liu, J. Gu, and S. Susstrunk. What is the space of spectral sensitivity functions for digital color cameras? In *IEEE Workshop on Applications of Computer Vision (WACV)*, pages 168–179, 2013.
- [9] R. Kawakami, H. Zhao, R. T. Tan, and K. Ikeuchi. Camera spectral sensitivity and white balance estimation from sky images. *International Journal of Computer Vision*, 105(3):187–204, 2013.
- [10] S. Quan. *Evaluation and optimal design of spectral sensitivities for digital color imaging*. PhD thesis, Rochester Institute of Technology, 2002.
- [11] P. Urban, M. Desch, K. Happel, and D. Spiehl. Recovering camera sensitivities using target-based reflectances captured under multiple LED-illuminations. In *Proceedings of the Workshop on Color Image Processing*, pages 9–16, 2010.
- [12] P. L. Vora, J. E. Farrell, J. D. Tietz, and D. H. Brainard. *Digital Color Cameras: Spectral Response*. Hewlett Packard Laboratories, 1997.
- [13] H. Zhao, R. Kawakami, R. T. Tan, and K. Ikeuchi. Estimating basis functions for spectral sensitivity of digital cameras. In *Meeting on Image Recognition and Understanding*, number 1, 2009.